European Journal of Medical Genetics 58 (2015) 492–496

Contents lists available at ScienceDirect

European Journal of Medical Genetics

journal homepage: http://www.elsevier.com/locate/ejmg

Clinical research

Leukoencephalopathy associated with 11q24 deletion involving the gene encoding hepatic and glial cell adhesion molecule in two patients

Toshiyuki Yamamoto [a, b, *], Shino Shimada [a, b], Keiko Shimojima [a], Noriko Sangu [a], Shinsuke Ninomiya [c], Masaya Kubota [d]

[a] Tokyo Women's Medical University Institute for Integrated Medical Sciences, Tokyo, Japan
[b] Department of Pediatrics, Tokyo Women's Medical University, Tokyo, Japan
[c] Department of Clinical Genetics, Kurashiki Central Hospital, Kurashiki, Japan
[d] Division of Neurology, National Center for Child Health and Development, Tokyo, Japan

ARTICLE INFO

Article history:
Received 8 February 2015
Accepted 15 June 2015
Available online 17 July 2015

Keywords:
Megalencephalic leukoencephalopathy with subcortical cysts type 2 (MLC2)
Hepatic and glial cell adhesion molecule (*HEPACAM*)
11q24
Microdeletion
Jacobsen syndrome

ABSTRACT

Leukoencephalopathies are heterogeneous entities with white matter abnormalities. Mutations of the gene encoding hepatic and glial cell adhesion molecule (*HEPACAM*) located on 11q24 are related to one of the leukoencephalopathies: megalencephalic leukoencephalopathy with subcortical cysts type 2 (MLC2). Genomic copy number aberrations were analyzed by microarray comparative hybridization for two patients. One patient who presented with abnormal intensity of the white matter had been previously been diagnosed with the typical genotype and phenotype of Jacobsen syndrome due to an 11q subtelomere deletion, which was further characterized here. In a second patient who exhibited the characteristic finding of leukoencephalopathy, an interstitial deletion of 11q24 was also identified. *HEPACAM* was involved in both deletions. We therefore suggest that haploinsufficiency of *HEPACAM*, a gene previously associated with the features of *MLC2* and located on the overlapping deletion region between the two patients, might be related to the observed white matter abnormalities.

1. Introduction

Leukoencephalopathies are heterogeneous entities characterized by white matter abnormalities (Schiffmann and van der Knaap, 2009). Leukoencephalopathies are generally diagnosed on the basis of their clinical course and neurological findings; however, the patterns of the neuroradiological findings serve as critical elements for ascertaining the specific diagnosis or disease classification (Schiffmann and van der Knaap, 2009). Megalencephalic leukoencephalopathy with subcortical cysts (MLC, MIM #604004) is one type of leukoencephalopathy wherein patients show early onset macrocephaly and delayed-onset neurological deterioration (van der Knaap et al., 1995). Typical patients with MLC show characteristic neuroradiological findings with subcortical cysts in the anterior-temporal region and/or in the frontoparietal region (van der Knaap et al., 2012). Cases of leukoencephalopathy associated with typical findings are relatively easily diagnosed, and 75% of patients with MLC show mutations in *MLC1* (MIM #605908), which is a major gene responsible for MLC that is located on chromosome 22q13.33 (Leegwater et al., 2001). Such molecular genetic evaluation is often required for the final diagnosis (Shimada et al., 2014). The remaining 25% of the patients manifesting the features of MLC show no mutation in *MLC1*, indicating genetic heterogeneity within the leukoencephalopathies. In 2011, the gene encoding the hepatic and glial cell adhesion molecule (*HEPACAM*, MIM #611642) was identified as the second gene associated with MLC features (Arnedo et al., 2014; Lopez-Hernandez et al., 2011a). HEPACAM and MLC1 both localize in axons and colocalize in the junctions between astrocytes, and HEPACAM has been shown to be required as a chaperon for proper localization of MLC1 and activation of volume-regulated anion currents (Capdevila-Nortes et al., 2013; Lopez-Hernandez et al., 2011b).

In this study, we identified two patients with white matter abnormalities associated with partial deletions of chromosome 11. We found that the shortest region of overlap (SRO) of both patients

* Corresponding author. Tokyo Women's Medical University Institute for Integrated Medical Sciences, 8-1 Kawada-cho, Shinjuku-ward, Tokyo 162-8666, Japan.
E-mail address: yamamoto.toshiyuki@twmu.ac.jp (T. Yamamoto).

http://dx.doi.org/10.1016/j.ejmg.2015.06.008
1769-7212/

included the *HEPACAM* locus. In addition, we discuss the functional relevance of haploinsufficiency of *HEPACAM* in these two patients in association with leukoencephalopathies.

2. Methods

This study was approved by the ethics committee in Tokyo Women's Medical University. After obtaining written informed consents from the patients' families, blood samples were obtained from the patients. Chromosomal microarray testing was performed using the Agilent 60K Human Genome CGH Microarray platform (Agilent Technologies, Santa Clara, CA, USA) according to the method described previously (Yamamoto et al., 2011, 2014). Sanger sequencing analysis for *MLC1* and for five genes encoding subunits of the eukaryotic translation initiation factor 2B (*EIF2B1*, *EIF2B2*, *EIF2B3*, *EIF2B4*, and *EIF2B5*) was performed for patient 2 in accordance with our previous studies (Shimada et al., 2012, 2014, 2015). The respective *HEPACAM* sequences were also analyzed by Sanger sequencing for both patients 1 and 2.

3. Results

3.1. Molecular cytogenetic analyses

The two patients reported in this study showed genomic copy number losses in 11q (Fig. 1). Patient 1 showed a subtelomeric deletion of 11q [arr 11q23.3q25(120,930,746–134,868,407) × 1]. The parents of this patient declined to be genotyped. Patient 2 showed an interstitial deletion of 11q [arr 11q23.3q24.2(119,982,356–125,310,469) × 1]. This region was not deleted in either parent of this patient, indicating *de novo* occurrence in patient 2. Additionally, patient 2 did not show any mutation in the coding regions of *MLC1*, *EIF2B1*, *EIF2B2*, *EIF2B3*, *EIF2B4*, and *EIF2B5*. No mutations were identified in the remaining allele of *HEPACAM* in either patient.

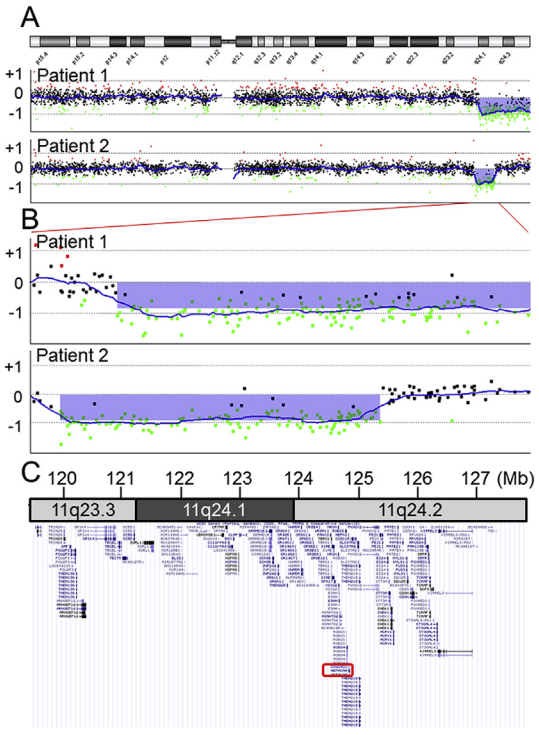

Fig. 1. Genome map of 11q and the results of chromosomal microarray testing. (A) The Chromosome View shows genomic copy number losses in the 11q24 regions in both patients. (B) The shortest region of overlap (SRO) is expanded in the Gene View. (C) Genome map in the same scale as shown in B. *HEPACAM* (red rectangle) is included in the SRO. (For interpretation of the references to colour in this figure legend, the reader is referred to the web version of this article.)

3.2. Patient reports

3.2.1. Patient 1

A 5-year-old girl was born with a birth weight of 1744 g (<3rd centile), a length of 41 cm (<3rd centile), and an occipitofrontal circumference (OFC) of 29.5 cm (3^{rd}–10th centile) at 37 weeks of gestation. Her Apgar score was 5/9 at 1/5 min. After birth, petechial spots were noted on her entire body. Blood examination revealed a low concentration of platelets (17,000/μl). No visceral anomaly was noted. In infancy, she showed delayed growth and development. She started walking without support at the age of 3 years and 5 months. At the age of 3 years and 8 months, her height was 84.5 cm (<3rd centile) and weight was 12.3 kg (10^{th}–25th centile). At that time, brain magnetic resonance imaging (MRI) revealed signal abnormalities in the white matter, predominantly in the deep white matter of the bilateral occipital lobes and faintly in the subcortical regions (Fig. 2). Conventional chromosomal analysis revealed an abnormal karyotype of 46,XX,del(11) (q23), indicating Jacobsen syndrome. Because the clinical features of the patient were compatible with those of Jacobsen syndrome, clinical diagnosis was confirmed.

At present, she still has not spoken meaningful words. The patient has a round face, short neck, bilateral ptosis, long philtrum, and thin upper vermilion. Laboratory examination has revealed her peripheral platelet level in the range of 10,000–80,000/μl.

3.2.2. Patient 2

A 20-month-old boy was born with a birth weight of 3105 g (50^{th}–75th centile), a length of 49.4 cm (50^{th}–75th centile), and an OFC of 36.0 cm (>97th centile) at 41 weeks of gestation, suggesting prenatal macrocephaly. He showed mild psychomotor developmental delay and could stand-up with support at 15 months of age. At present, he can walk with support and can speak only some decipherable words. He shows no distinctive features except for left ptosis and right cryptorchidism. His OFC is 49 cm (50^{th}–75th centile), indicating improvement upon his initial macrocephaly. Brain MRI examination at 20 months of age revealed signal abnormalities remarkably in the subcortical regions rather than in the deep white matter (Fig. 2).

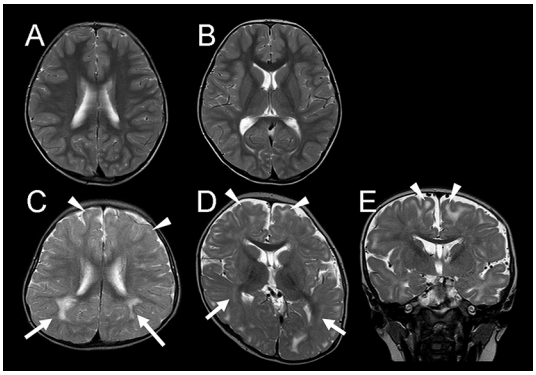

Fig. 2. Brain MRI findings of the patients reported in this study. (A and B) The T2-weighted axial images of a normally developing 4-year-old boy, who was examined for the aim of the disease screening for epilepsy, with normal MRI results. (C) The T2-weighted axial image of patient 1 examined at 3 years and 8 months of age. (D, E) The T2-weighted axial (D) and coronal (E) images of patient 2 examined at 20 months of age. Compared to the normal control (A, B), both patients show T2-high intensities in their deep (arrows) and subcortical (arrow heads) white matter.

Table 1
Gene information included in the deletion region of the patients.

Gene symbol	Gene/Locus MIM number	Description	Position[a]	Phenotype MIM number	Phenotype	Deletion region of the patients
TRIM29	#610658	tripartite motif containing 29	119,981,994–119,992,701			Patient 2
OAF		OAF homolog (Drosophila)	120,081,747–120,100,650			
POU2F3	#607394	POU class 2 homeobox 3	120,107,349–120,190,653			
TMEM136		transmembrane protein 136	120,195,838–120,204,388			
ARHGEF12	#604763	Rho guanine nucleotide exchange factor (GEF) 12	120,207,618–120,360,645			
GRIK4	#600282	glutamate receptor, ionotropic, kainate 4	120,530,978–120,856,969			
TBCEL	#610451	tubulin folding cofactor E-like	120,894,803–120,960,354			
TECTA	#602574	tectorin alpha	120,973,375–121,061,515	#601543	Deafness, autosomal dominant 8/12	Patient 1
				#603629	Deafness, autosomal recessive 21	
SC5D	#602286	sterol-C5-desaturase	121,163,388–121,184,119	#607330	Lathosterolosis	
SORL1	#602005	sortilin-related receptor, L(DLR class) A repeats containing	121,322,912–121,504,471	#104300	Association with Alzheimer disease	
BLID	#608853	BH3-like motif containing, cell death inducer	121,986,062–121,986,923			
UBASH3B	#609201	ubiquitin associated and SH3 domain containing B	122,526,398–122,685,187			
CRTAM	#612597	cytotoxic and regulatory T cell molecule	122,709,255–122,743,347			
C11orf63		chromosome 11 open reading frame 63	122,753,236–122,830,430			
BSX	#611074	brain-specific homeobox	122,848,357–122,852,379			
HSPA8	#600816	heat shock 70 kDa protein 8	122,928,200–122,931,094			
CLMP	#611693	CXADR-like membrane protein	122,943,033–123,066,007	#615237	Congenital short bowel syndrome	
GRAMD1B		GRAM domain containing 1B	123,396,528–123,493,518			
SCN3B	#608214	sodium channel, voltage-gated, type III, beta subunit	123,499,895–123,525,315	#613120	Atrial fibrillation, familial, 16	
				#613120	Brugada syndrome 7	
ZNF202	#603430	zinc finger protein 202	123,594,997–123,612,363			
OR6X1		olfactory receptor, family 6, subfamily X, member 1	123,624,288–123,625,226			
TMEM225		transmembrane protein 225	123,753,633–123,756,340			
OR8D4		olfactory receptor, family 8, subfamily D, member 4	123,777,139–123,778,083			
OR4D5		olfactory receptor, family 4, subfamily D, member 5	123,810,324–123,811,280			
OR6T1		olfactory receptor, family 6, subfamily T, member 1	123,813,574–123,814,545			
OR10S1		olfactory receptor, family 10, subfamily S, member 1	123,847,403–123,848,398			
OR10G4		olfactory receptor, family 10, subfamily G, member 4	123,886,282–123,887,217			
OR10G9		olfactory receptor, family 10, subfamily G, member 9	123,893,720–123,894,655			
OR10G8		olfactory receptor, family 10, subfamily G, member 8	123,900,330–123,901,265			
OR10G7		olfactory receptor, family 10, subfamily G, member 7	123,908,773–123,909,708			
VWA5A	#602929	Willebrand factor A domain containing 5A	123,986,111–124,017,618			
OLFR959		NI	124,029,125–124,029,838			
OR10D3		NI	124,055,975–124,056,912			
OR8G2		olfactory receptor, family 8, subfamily G, member 2	124,095,398–124,096,312			
OR8G1		olfactory receptor, family 8, subfamily G, member 1	124,120,423–124,135,763			
OR8D1		olfactory receptor, family 8, subfamily D, member 1	124,179,736–124,180,662			
OR8D2		olfactory receptor, family 8, subfamily D, member 2	124,189,158–124,190,093			
OR8B2		olfactory receptor, family 8, subfamily B, member 2	124,252,298–124,253,239			
OR8B3		olfactory receptor, family 8, subfamily B, member 3	124,266,306–124,267,247			
OR8B4		olfactory receptor, family 8, subfamily B, member 4	124,293,838–124,294,767			
OR8B8		olfactory receptor, family 8, subfamily B, member 8	124,310,046–124,310,981			
OR8B12		olfactory receptor, family 8, subfamily B, member 12	124,412,618–124,413,550			
OR8A1		olfactory receptor, family 8, subfamily A, member 1	124,439,965–124,440,945			
PANX3	#608422	pannexin 3	124,481,453–124,490,251			
TBRG1	#610614	transforming growth factor beta regulator 1	124,492,742–124,505,822			
SIAE	#610079	sialic acid acetylesterase	124,505,685–124,543,777	#613551	Autoimmune disease susceptibility	
SPA17	#608621	sperm autoantigenic protein 17	124,543,740–124,564,687			
NRGN	#602350	neurogranin (protein kinase C substrate, RC3)	124,609,829–124,617,102			
VSIG2	#606011	V-set and immunoglobulin domain containing 2	124,617,370–124,622,109			
ESAM	#614281	endothelial cell adhesion molecule	124,623,019–124,632,223			
MSANTD2		Myb/SANT-like DNA-binding domain containing 2	124,636,394–124,670,299			
ROBO3	#608630	roundabout, axon guidance receptor, homolog 3 (Drosophila)	124,735,305–124,751,370	#607313	Gaze palsy, horizontal, with progressive scoliosis	

ROBO4	#607528	roundabout, axon guidance receptor, homolog 4 (Drosophila)	124,754,114–124,767,831			
HEPN1	#611641	hepatocellular carcinoma, down-regulated 1	124,789,146–124,790,573			
HEPACAM	#611642	hepatic and glial cell adhesion molecule	124,789,146–124,806,308	#613925	Megalencephalic leukoencephalopathy with subcortical cysts 2A	
				#613926	Megalencephalic leukoencephalopathy with subcortical cysts 2B, remitting, with or without mental retardation	
CCDC15		coiled-coil domain containing 15	124,824,017–124,911,385			
SLC37A2		solute carrier family 37 (glycerol-3-phosphate transporter), member 2	124,933,013–124,960,412			
TMEM218		transmembrane protein 218	124,964,266–124,981,604			
PKNOX2	#613066	PBX/knotted 1 homeobox 2	125,034,559–125,303,285			

[a] Genomic position on the chromosome 11 referring to the GRCh37 build reference sequence (hg19); NI, no information.

4. Discussion

In this study, we identified two overlapping chromosomal deletions of 11q associated with white matter abnormalities. Patient 1 showed a subtelomeric deletion of 11q, which is a typical pattern for Jacobsen syndrome. Patients with typical features of Jacobsen syndrome show intellectual disability, short stature, congenital heart defects, thrombocytopenia, and characteristic facial features (Grossfeld et al., 2004; Mattina et al., 2009; Takahashi et al., 2012). Although patient 1 did not show congenital heart defects, the incidence of congenital heart defects in Jacobsen syndrome is not 100% (Wenger et al., 2006). Therefore, clinical features of patient 1 fulfilled the diagnostic criteria for Jacobsen syndrome. Patient 2 showed an interstitial deletion of 11q. Although this patient showed mild developmental delay, he exhibited no other clinical feature distinctive of Jacobsen syndrome. Therefore, patient 2 did not satisfy the diagnostic criteria for this syndrome (Mattina et al., 2009).

Both patients showed neuroradiological abnormalities in the deep and subcortical white matter regions, albeit with different patterns. In patient 1, the main white matter abnormality is observed in the deep white matter, especially in the bilateral occipital lobes, as detected by the T2-weigthed MRI (Fig. 2C). In addition to that, signal abnormalities can be detected also in the subcortical white matter regions. In patient 2, white matter abnormalities are remarkable in the subcortical white matter regions rather than in the deep white matter regions (Fig. 2). Although subcortical cysts were not clearly detected in both patients, the distribution of white matter abnormalities was similar to that seen in the early stage of MLC. Macrocephaly observed in early infantile period of patient 2 is also a suggestive feature of MLC.

We identified a 5.3 Mb region of 11q23.3q24.2 that was deleted in patient 2. Of the genes included in the deletion region, nine genes are registered as disease-causing genes in the database online Mendelian inheritance in men (OMIM), i.e., *ARHGEF12*, *TECTA*, *SC5D*, *SORL1*, *CLMP*, *SCN3B*, *SIAE*, *ROBO3*, and *HEPACAM* (Table 1). Among these, *HEPACAM* has been shown to be associated with megalencephalic leukoencephalopathy with subcortical cysts-2A (MLC2A; MIM# 613925) and B (MLC2B; MIM# 613926) (Lopez-Hernandez et al., 2011a). Furthermore, *HEPACAM* mutations have been shown to exert novel, dual effects including both autosomal recessive (MLC2A) and autosomal dominant (MLC2B) patterns (Arnedo et al., 2014). Patients with *HEPACAM* mutations in an autosomal recessive fashion show classical phenotypes with infantile-onset macrocephaly, delayed-onset motor deterioration, epilepsy, and cognitive decline of variable severity, which are associated with white matter abnormalities (MLC2A) (Lopez-Hernandez et al., 2011a). In comparison, patients with *HEPACAM* mutations inherited in an autosomal dominant fashion have also been reported who show macrocephaly within the first year of life; however, the motor capabilities in these patients were rarely impaired. Furthermore, white matter abnormalities detected upon initial examination of these patients showed improvement upon follow-up; this pattern is classified as MLC2B (Arnedo et al., 2014). Dominantly inherited *HEPACAM* mutations have been reported to often cause benign familial macrocephaly or macrocephaly with intellectual disability and/or autism. However, because the previously reported *HEPACAM* mutations related to MLC2B consisted of missense mutations in the specific domain required for interaction with *MLC1* (Lopez-Hernandez et al., 2011a), it is reasonable to suspect that the underlying mechanism of MLC2B in these patients might be related to dominant-negative effects. Macrocephaly has also been reported in one of the parents of a patient with MLC2A who carried a loss-of-function mutation (Lopez-Hernandez et al., 2011a), indicating that both *HEPACAM* haploinsufficiency as well

as mutation might cause macrocephaly. Because we were unable to identify a *HEPACAM* mutation in the remaining allele of patient 2, we assume that haploinsufficiency of *HEPACAM* is the only mechanism related to macrocephaly and white matter abnormalities in this patient. Macrocephaly of patient 2 was identified at birth, but has improved at 20 months; it is unclear whether the white matter abnormalities might improve as well, as do those of patients with *HEPACAM* mutations rather than deletions.

Although most of the deletion regions identified in patients with Jacobsen syndrome include *HEPACAM*, no previous patient with Jacobsen syndrome has been reported to show an MLC-like phenotype. However, some of the previously reported patients with Jacobsen syndrome have shown related findings. For example, Ono et al. reported two patients with 11q deletions associated with delayed myelination, suspected by the abnormal signal intensities revealed by MRI (Ono et al., 1994). In addition, Grossfeld et al. reported that abnormal brain imaging findings were identified in 24/47 (51%) of patients with Jacobsen syndrome (Grossfeld et al., 2004). The result of the present study provide additional insight into these findings: we identified a patient with Jacobsen syndrome (patient 1) associated with white matter abnormalities, although the identified distributions were different from those observed in patient 2. *HEPACAM* was included in the SRO of both patients, we considered that haploinsufficiency of *HEPACAM* might therefore cause white matter abnormalities to varying degrees. We suggest that the improvement of phenotype overtime, or a low penetrance of white matter abnormalities consequent to *HEPACAM* deletion might, among other factors, contribute to the lack of descriptions of MLC-like phenotypes in patients with Jacobsen syndrome to date.

In addition, it is likely that the developmental delay observed in patient 2 could have been modified by the loss of neighboring genes included in the deletion region. In 2009, Coldren et al. analyzed genotype–phenotype correlations for 14 patients with Jacobsen syndrome and suggested that two genes, the brain-specific homeobox gene (*BSX*) and the neurogranin gene (*NRGN*), might be possible candidate genes for global and selective deficits in neurocognitive functions (Coldren et al., 2009). Because both of these genes are also included in the SRO identified in this study (Table 1), haploinsufficiencies of these two genes in particular might have modified neurodevelopment in patient 2 as well.

In conclusion, we report the characterization of two patients with white matter abnormalities in association with 11q24 deletions involving *HEPACAM*. This finding suggests that haploinsufficiency of *HEPACAM* might be related to white matter abnormalities. Further studies are required to obtain more information on white matter abnormalities in patients with 11q24 deletions in order to confirm the results of this study.

Conflict of interest

The authors have no conflict of interests to declare.

Acknowledgment

We thank the patients and their families for cooperation in this study. We would like to acknowledge the Collaborative Research Supporting Committee of the Japanese Society of Child Neurology (14-3) for promoting this study. This work was supported by a Grant-in-Aid for Scientific Research from Health Labor Sciences Research Grants from the Ministry of Health, Labor, and Welfare, Japan (T.Y.).

References

Arnedo, T., Aiello, C., Jeworutzki, E., Dentici, M.L., Uziel, G., et al., 2014. Expanding the spectrum of megalencephalic leukoencephalopathy with subcortical cysts in two patients with GLIALCAM mutations. Neurogenetics 15, 41–48.

Capdevila-Nortes, X., Lopez-Hernandez, T., Apaja, P.M., Lopez de Heredia, M., Sirisi, S., et al., 2013. Insights into MLC pathogenesis: GlialCAM is an MLC1 chaperone required for proper activation of volume-regulated anion currents. Hum. Mol. Genet. 22, 4405–4416.

Coldren, C.D., Lai, Z., Shragg, P., Rossi, E., Glidewell, S.C., et al., 2009. Chromosomal microarray mapping suggests a role for BSX and neurogranin in neurocognitive and behavioral defects in the 11q terminal deletion disorder (Jacobsen syndrome). Neurogenetics 10, 89–95.

Grossfeld, P.D., Mattina, T., Lai, Z., Favier, R., Jones, K.L., et al., 2004. The 11q terminal deletion disorder: a prospective study of 110 cases. Am. J. Med. Genet. A 129A, 51–61.

Leegwater, P.A., Yuan, B.Q., van der Steen, J., Mulders, J., Konst, A.A., et al., 2001. Mutations of MLC1 (KIAA0027), encoding a putative membrane protein, cause megalencephalic leukoencephalopathy with subcortical cysts. Am. J. Hum. Genet. 68, 831–838.

Lopez-Hernandez, T., Ridder, M.C., Montolio, M., Capdevila-Nortes, X., Polder, E., et al., 2011. Mutant GlialCAM causes megalencephalic leukoencephalopathy with subcortical cysts, benign familial macrocephaly, and macrocephaly with retardation and autism. Am. J. Hum. Genet. 88, 422–432.

Lopez-Hernandez, T., Sirisi, S., Capdevila-Nortes, X., Montolio, M., Fernandez-Duenas, V., et al., 2011. Molecular mechanisms of MLC1 and GLIALCAM mutations in megalencephalic leukoencephalopathy with subcortical cysts. Hum. Mol. Genet. 20, 3266–3277.

Mattina, T., Perrotta, C.S., Grossfeld, P., 2009. Jacobsen syndrome. Orphanet J. Rare Dis. 4, 9.

Ono, J., Harada, K., Hasegawa, T., Sakurai, K., Kodaka, R., et al., 1994. Central nervous system abnormalities in chromosome deletion at 11q23. Clin. Genet. 45, 325–329.

Schiffmann, R., van der Knaap, M.S., 2009. Invited article: an MRI-based approach to the diagnosis of white matter disorders. Neurology 72, 750–759.

Shimada, S., Miya, K., Oda, N., Watanabe, Y., Kumada, T., et al., 2012. An unmasked mutation of EIF2B2 due to submicroscopic deletion of 14q24.3 in a patient with vanishing white matter disease. Am. J. Med. Genet. A 158A, 1771–1777.

Shimada, S., Shimojima, K., Masuda, T., Nakayama, Y., Kohji, T., et al., 2014. MLC1 mutations in Japanese patients with megalencephalic leukoencephalopathy with subcortical cysts. Hum. Genome Var. 1, 14019.

Shimada, S., Shimojima, K., Sangu, N., Hoshino, A., Hachiya, Y., et al., 2015. Mutations in the genes encoding eukaryotic translation initiation factor 2B in Japanese patients with vanishing white matter disease. Brain Dev. http://dx.doi.org/10.1016/j.braindev.2015.03.003 (in press).

Takahashi, I., Takahashi, T., Sawada, K., Shimojima, K., Yamamoto, T., 2012. Jacobsen syndrome due to an unbalanced translocation between 11q23 and 22q11.2 identified at age 40 years. Am. J. Med. Genet. A 158A, 220–223.

van der Knaap, M.S., Barth, P.G., Stroink, H., van Nieuwenhuizen, O., Arts, W.F., et al., 1995. Leukoencephalopathy with swelling and a discrepantly mild clinical course in eight children. Ann. Neurol. 37, 324–334.

van der Knaap, M.S., Boor, I., Estevez, R., 2012. Megalencephalic leukoencephalopathy with subcortical cysts: chronic white matter oedema due to a defect in brain ion and water homoeostasis. Lancet Neurol. 11, 973–985.

Wenger, S.L., Grossfeld, P.D., Siu, B.L., Coad, J.E., Keller, F.G., et al., 2006. Molecular characterization of an 11q interstitial deletion in a patient with the clinical features of Jacobsen syndrome. Am. J. Med. Genet. A 140, 704–708.

Yamamoto, T., Shimojima, K., Nishizawa, T., Matsuo, M., Ito, M., et al., 2011. Clinical manifestations of the deletion of down syndrome critical region including DYRK1A and KCNJ6. Am. J. Med. Genet. A 155A, 113–119.

Yamamoto, T., Wilsdon, A., Joss, S., Isidor, B., Erlandsson, A., et al., 2014. An emerging phenotype of Xq22 microdeletions in females with severe intellectual disability, hypotonia and behavioral abnormalities. J. Hum. Genet. 59, 300–306.